

Assessment of Power System Stability Considering Multiple Time-Scale Dynamics: Insights into Hopf Bifurcations in Presence of GFL and GFM IBRs

Luis David Pabón Ospina
Grid Control and Grid Dynamics
Fraunhofer IEE
Kassel, Germany
luis.david.pabon.ospina@iee.fraunhofer.de

Abstract—Real power systems exhibit dynamics that evolve across a wide range of time scales, from very fast to very slow phenomena. Historically, incorporating these wide-ranging dynamics into a single model has been impractical. As a result, power engineers rely on time-scale decomposition to simplify models. When fast phenomena are evaluated, slow dynamics are neglected (assumed stable), and vice versa. This paper challenges this paradigm by showing the importance of assessing power system stability while considering multiple time scales simultaneously. Using the concept of Hopf bifurcations, it exemplifies instability issues that would be missed if multi-time-scale dynamics are not considered. Although this work employs both grid-following and grid-forming inverter-based resource models, it is not a direct comparison. Instead, it presents a case study demonstrating how one technology can complement the other from a multi time-scale dynamics perspective.

Index Terms—Forced Oscillations, Grid-Forming IBR, Grid-Following IBR, Inverter-Based Generation, Low-Inertia Networks.

I. INTRODUCTION

Even in traditional power systems without Inverter-Based Resources (IBRs), it was impractical to incorporate dynamics from a wide range of time scales into a single model. For example, when assessing rotor angle stability, it was (and still is) common practice to consider only the dynamics in the time scale of electromechanical oscillations. Models for Automatic Voltage Regulators (AVR), Speed Governors (GOV), and Power System Stabilizers (PSS) were typically considered in these studies, with simulations usually running for 10 seconds or less. Slower dynamics, such as load restoration processes via Automatic Load Tap Changers (LTCs) and the action of Over-Excitation Limiters (OELs), which act over tens of seconds or minutes, were usually neglected.

While this is a reasonable approach in some cases, time-scale decomposition is often performed by system operators

and utilities intuitively with little to no mathematical rigor. Nevertheless, power systems have interdependent dynamics across multiple time scales. This interdependency means that behavior from one time scale can cause issues in another. A strong example of this is provided in Chapter 8.2.3 of [1], which discusses short-term instability induced by long-term dynamics. In this case, the evolution of unstable slow variables leads to a short-term instability. The text distinguishes three types of such instability:

- S-LT1: The loss of short-term equilibrium caused by long-term dynamics. A typical example is the loss of synchronism of a synchronous generator after its OEL has limited the field current. This often results in an exponential collapse, similar to a saddle-node bifurcation or a purely real unstable eigenvalue. An example of this was illustrated in [2] by the author.
- S-LT2: The loss of attraction to the stable short-term equilibrium due to a shrinking region of attraction caused by long-term dynamics.
- S-LT3: The oscillatory instability of short-term dynamics caused by long-term dynamics.

The last of these, S-LT3, is the main focus of this paper. In traditional systems, S-LT3 was plausible but rare. One possible scenario involved the OEL limiting the field current, which could inactivate the PSS that relies on the field current for its stabilizing action [3]. This paper demonstrates that oscillatory instability resulting from a Hopf bifurcation induced by long-term dynamics can be a significant threat in modern power systems with IBRs.

II. BRIEF RECAP OF NONLINEAR DYNAMICS CONCEPTS

A. Stable Manifolds

Let us consider the following dynamical system,

$$\dot{x} = f(x, y) \quad (1)$$

$$\epsilon \dot{y} = g(x, y) \quad (2)$$

This work was supported in part by the German Ministry for Economic Affairs and Energy, in part by the Projektträger Jülich under Projects LISA -FKZ03EI4059A and SysStab2023 -FKZ03EI6122H. Only the authors are responsible for the content of this publication.

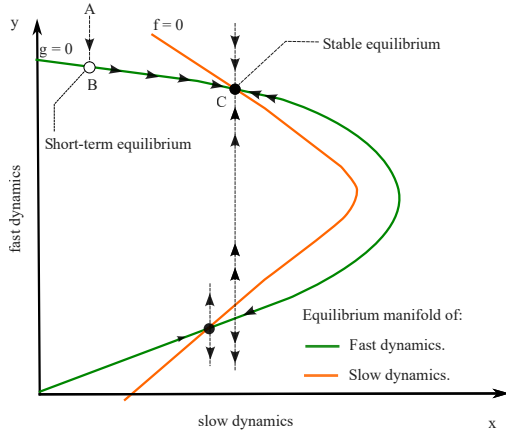


Fig. 1. Equilibrium manifolds that intercept - modified from [4].

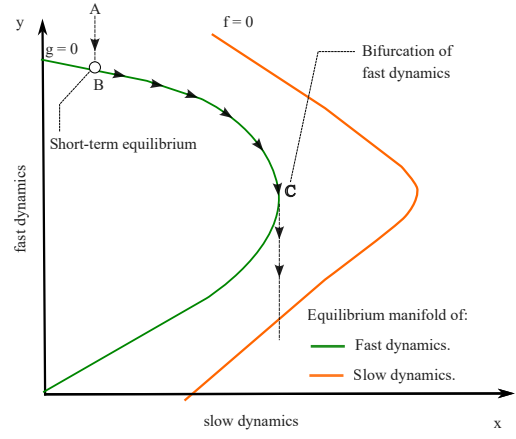


Fig. 2. Equilibrium manifolds that don't intercept - modified from [4].

where x is the “slow” state vector that contains all slow dynamics, y represents the “fast” state vector, and ϵ is a small parameter. The stable manifold is defined as the set of initial conditions x_0 such that $\mathbf{x}(t) \rightarrow \mathbf{x}^*$ as $t \rightarrow \infty$, where \mathbf{x}^* is a fixed (or equilibrium) point. The same applies to the fast state vector. This is easily illustrated using Fig. 1 which is modified from [4].

Consider that the system is operating at point A. If a disturbance occurs, such as a short circuit followed by a line trip, the system will rapidly transition from point A to point B, which lies on the fast dynamics equilibrium manifold (green curve), defined by $g = 0$ in (2). Point B represents a short-term equilibrium in which only fast dynamics are at a fixed point. After some time, the slow dynamics begin to influence the system, slowly drawing it towards the slow dynamics equilibrium manifold (orange curve). Eventually, the system reaches point C, where both f and g are zero in (1) and (2). This represents the true equilibrium of the system [2].

Nevertheless, both equilibrium manifolds don't always intercept like it is shown in Fig. 2. In this case, the system will quickly transition from A to B, settling into a short-term equilibrium. Eventually, the slow dynamics act and push the system towards the slow dynamics equilibrium manifold. Before the system can settle into a point where $f = 0$, there is a bifurcation of the fast dynamics at point C and the system becomes unstable.

B. Bifurcations and Limit Cycles

In dynamical systems, equilibrium points can be created or destroyed, or their stability can change. These qualitative changes in the dynamics are called bifurcations, and the parameter values at which they occur are known as bifurcation points [5]. In power system dynamics, two types of bifurcations are common:

1) *Saddle-Node bifurcation (SNB)*: Occurs when a system's equilibria are suddenly created or destroyed as a parameter changes. This phenomenon is often seen in power systems, such as the SNB of PV curves. From a stability perspective,

this represents an eigenvalue of the state matrix crossing the imaginary axis at the origin (no imaginary part).

2) *Hopf bifurcation*: Requires a system of at least two dimensions. It happens when a stable fixed point loses its stability and gives rise to a stable, periodic oscillation known as a *limit cycle*. This is a mechanism by which a system can transition from a steady state to an oscillating state. This transition is represented by a pair of complex conjugate eigenvalues of the state matrix crossing the imaginary axis. Reference [6] explores the relevance of fast line dynamics for this type of bifurcation.

3) *Limit cycle*: An isolated closed trajectory in the *phase plane*. If all neighboring trajectories approach the limit cycle, it is considered stable or attracting. Otherwise it is considered unstable. In power system dynamics, limit cycles appear as undamped oscillations of physical quantities like voltage or power.

4) *Phase plane*: Graphical representation of a dynamical system's behavior, where the state variables are plotted on the axes. A point on the phase plane corresponds to a specific state of the system at a particular moment in time. All possible trajectories, or *phase portrait*, drawn on this plane illustrate how the system evolves over time from different initial conditions.

III. TEST SYSTEM AND DYNAMIC MODELS

The test system and the dynamic models used in this work are well-known, well-established, and publicly available. Consequently, this section will describe only the key characteristics and any modifications that were made.

A. Test System

The IEEE Nordic Test System, detailed in [7], [8], is employed in this work due to its consideration of dynamics across various timescales. It includes typical fast-acting components like AVR and PSSs, as well as slower-acting equipment such as OELs and LTCs. The system is publicly available in multiple formats on the IEEE PSDP website [9]. Two modifications were made to the test system. First,

the synchronous generators g6 and g7 in the central area were replaced by Grid-Following (GFL) PV plants, sized at 400 MVA and 200 MVA respectively. These will be referred to as IBR_6 and IBR_7. Second, a 100 MVA Grid-Forming battery was considered at bus 1042, which is the same bus where IBR_6 is connected, but only for one study case.

B. GFL IBR Model

Inspired by the Western Electric Coordinating Council (WECC) REGC_C model [10], [11], which is widely available in several software tools. Key features of this model relevant to this work include the consideration of both PLL and inner current control dynamics. For more insights into the model's structure and its applicability to the phenomena discussed in this publication, refer to the author's previous works [12], [13]. In addition to the inner control, the outer control REEC_B and plant control REPC_A models were also considered. These models have been developed and validated by the members of the WECC Model Validation Subcommittee (MVS).

C. GFM IBR Model

The well-established WECC REGFM_A1 model is used in this work. According to [14], the model's development was a collaborative effort between the Pacific Northwest National Laboratory's (PNNL) Directed Research and Development program and the Universal Interoperability for Grid-Forming Inverters (UNIFI) consortium. This positive-sequence model is capable of representing the characteristics of droop-controlled GFM IBRs and has been approved by the WECC Model Validation Subcommittee for use in interconnection-wide studies within the WECC. The model was created through collaboration between PNNL, EPRI, and SMA Solar Technology. Details can be found in [15].

IV. SIMULATION RESULTS

One of the primary characteristics of the test system used in this work is the high power transfer from the North to the Central area. Under these conditions, the tripping of a transmission line, such as Line 4032-4044, can lead to long-term instability or collapse. This is a phenomenon that can be attributed mainly to slow dynamics, starting with the action of LTCs to control distribution voltages, which attempts to restore load consumption towards the pre-disturbance value which is unfeasible after the line trip. To control voltage, synchronous machines in the Central region increase their field current which eventually leads to the action of their OEL that limits the field current to protect the generator windings. These generators lose their voltage control capability. Depending on the considered scenario, the system reaches either instability, e.g., unacceptable low voltages, sustained oscillations, etc. or collapse, which is an abrupt fall of voltages resulting in a system blackout [7]. For this reason, this study investigates the tripping of said line as the primary event.

Four cases are presented in this work and are summarized in Table I.

TABLE I
STUDY CASES

Case	Case 1	Case 2	Case 3	Case 4
GFL PV (IBGs 6 and 7)	Yes	Yes	Yes	Yes
PLL Bandwidth in Hz	8	8	4	8
Voltage Emergency Control	No	Yes	Yes	Yes
GFM Battery	No	No	No	Yes

The "Voltage Emergency Control" in Table I corresponds to a typical countermeasure often implemented as conservation voltage reduction (CVR). This technique mitigates emergencies by reducing the voltage setpoint of LTCs to a predefined value, for example, 0.95 pu. This action takes advantage of the voltage sensitivity of residential loads to lower consumption during an emergency. While traditional methods use fixed voltage reductions, more advanced approaches exist, such as the one presented by the authors in [16] and patented in Europe and the U.S. [17]. These methods offer a less intrusive scheme where the distribution voltage is not decreased by a fixed value. Activation of these emergency controls can be triggered by monitoring transmission voltage thresholds or, more effectively, by applying advanced methods like Local Identification of Voltage Emergency Situations (LIVES) or "New LIVES" index [18].

A. Case 1 - GFL (Fast PLL) Without Voltage Emergency Control

The evolution of transmission voltages after the contingency is presented in Fig. 3, which concludes that:

- Despite the generating units' control efforts, the voltage cannot be restored to its pre-disturbance value.
- An undamped oscillation is already visible in the transmission voltages. This oscillation is more pronounced in the power output of IBRs, as will be shown shortly.
- The system ends up operating in a state where some synchronous generators have lost their voltage control capabilities. A critical event happens shortly before 200 s, when the OEL of generator g14 in the central area acts.

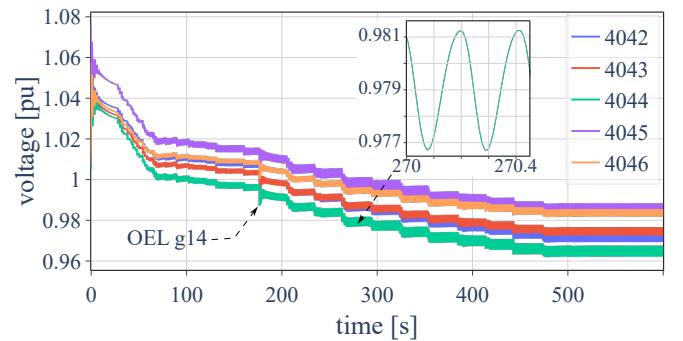


Fig. 3. Evolution of Transmission Voltages - Case 1.

The observed undamped oscillation is not a direct consequence of the initial contingency; instead, it is induced by unstable slow dynamics (S-TL3). This can be explained using Fig. 4, which shows the behavior after short-term equilibrium. The figure contains substantial information and requires a step-by-step explanation. Let's focus on the two axes where the PLL states of IBR_6 are plotted. The state x_1 is associated with the proportional-integral controller, which is standard in most synchronous-reference frame PLLs (the block diagram can be found in [12]). The state x_2 represents the estimated voltage phase. Plotting these two states provides a phase plane for the PLL dynamics. After the contingency, these states oscillate but quickly settle to a short-term equilibrium, which is marked in the figure. This would correspond to point **B** in Fig. 2.

Let us now focus on the “Load Central Zone [MW]” axis. The original load consumption (before the contingency) is marked with a red line shortly before 5820 MW. When the system finds the aforementioned short-term equilibrium after the fault, the load consumption has been reduced to around 5700 MW (marked with a dashed line). The overall effect of slow dynamics led by LTC actions is to slowly restore the load from the dashed line towards the red line in Fig. 4. This is the equivalent of traveling from point **B** in Fig. 1 or Fig. 2 towards the slow dynamics equilibrium manifold (exemplified with the orange line). In this case, the fast PLL dynamics lose stability as the system travels towards the slow dynamics equilibrium manifold (as in Fig. 2). The PLL dynamics encounter a *Hopf* bifurcation that gives birth to a stable limit cycle on the PLL states phase plane. The oscillatory behavior becomes more pronounced the more the load consumption of the central zone is restored. As previously mentioned, there is an interesting event shortly before 200 s.

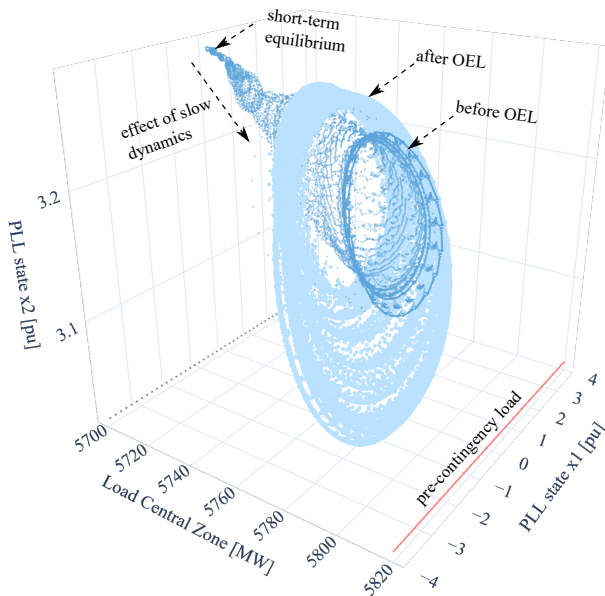


Fig. 4. Phase-space Trajectory - Case 1.

The OEL of synchronous machine g14 in the affected area operates. This inhibits the voltage control capability of the generator, further hindering the stability of the system. This is the reason why Fig. 4 has two shades of blue. The evolution of the PLL states before the OEL of g14 acts is shown with dark blue. After the OEL action, the trace is shown with light blue. This is to show the significant effect that the OEL action has on the stability of faster PLL dynamics. Two things can be highlighted after the OEL action. First, the oscillatory behavior becomes even more evident with an even “bigger” limit cycle. Second, the active power of the central zone is slightly reduced. This is due to the voltage dependency of loads after voltages in the central area are reduced due to the OEL action.

Figure 4 might be unconventional in the power system dynamics community, but it reveals the intrinsic interactions between slow and fast dynamics. The S-LT3 instability leads to undamped oscillations in the IBR power output, which is visible in Figs. 5 and 6.

Note that the S-LT3 instability captured in this section would be missed if multi-time-scale dynamics are not considered. To corroborate this, Fig. 7 presents the case in which the PLL and the inner current control of IBRs are modeled. These are thought to be the key elements in capturing such forced oscillations. Nevertheless, the slow dynamic components (LTCs, OELs, etc.) will not be modeled.

The conclusion is clear: even though the fast IBR dynamics were modeled, no oscillations were captured. This is because there are no mechanisms that make the system travel towards

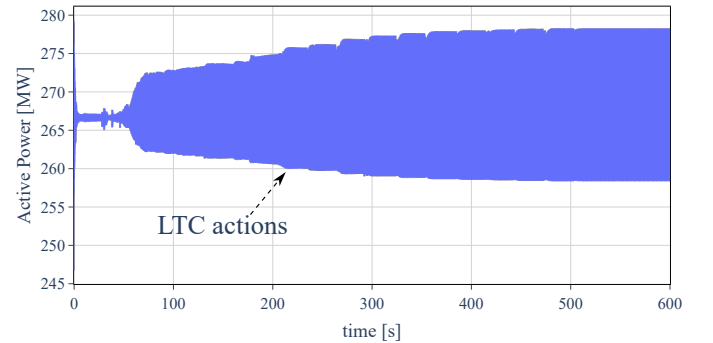


Fig. 5. IBG_6 Active Power - Case 1.

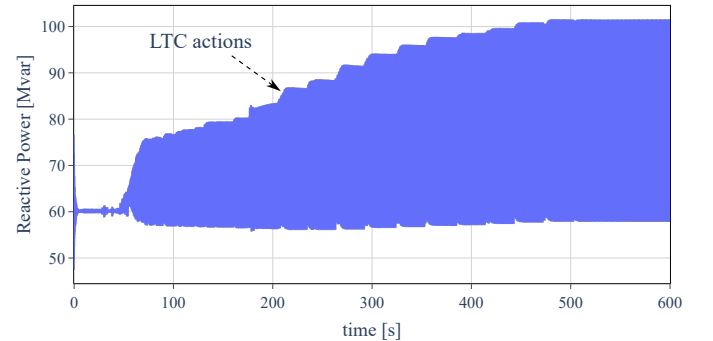


Fig. 6. IBG_6 Reactive Power - Case 1.

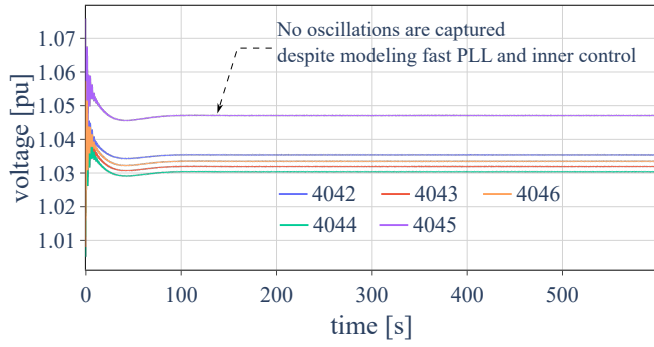


Fig. 7. Results Without Considering Multi-time-scale Dynamics.

the slow dynamics equilibrium manifold. In other words, the system will remain at point **B** of Fig. 2, giving a false sense of a stable equilibrium. Only when the slow and fast dynamics are modeled together do the interactions between both time scales become evident and the S-LT3 instability is detected.

B. Case 2 - GFL (Fast PLL) With Voltage Emergency Control

The S-LT3 instability presented in the previous section has two issues that need to be corrected. First, the voltages should be recovered and the system stress needs to be relieved so that synchronous generators can regain their voltage control capability instead of being limited by their OEL. Second, the undamped oscillations need to be mitigated. Case 2 addresses the first issue. To do this, a classical CVR scheme is applied in which the voltage setpoint of LTCs is reduced by 5% at $t = 300s$. The effect of such control can be observed in Fig. 8.

Figure 9 presents the PLL phase plane together with the active power consumption in the Central zone. Note that the trace has two shades of blue. All results before the CVR scheme at $t = 300s$ are shown in dark blue. The slow dynamics again cause an increase in active power in the central area, from the dashed line (before 5700 MW) to the red line (after 5800 MW). The fast dynamics of the PLL oscillate exactly as shown in the previous section. The difference starts at $t \geq 300s$ when the CVR is activated. The results for this period are shown with a light blue trace. The CVR scheme reduces the power consumption as indicated by the direction arrow labeled “Effect of emergency control” in Fig. 9. As the

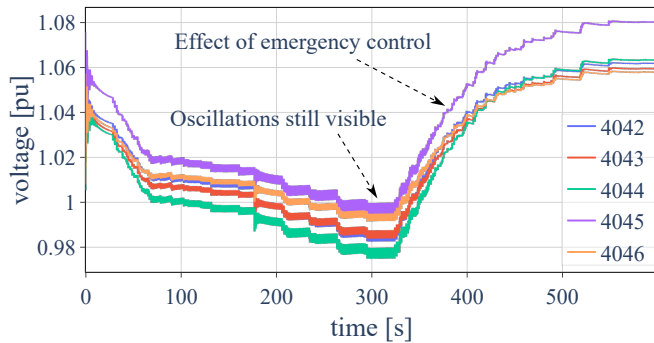


Fig. 8. Evolution of Transmission Voltages - Case 2.

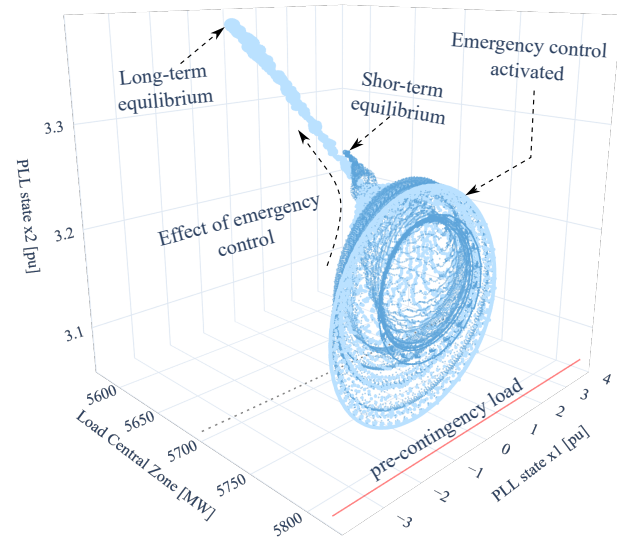


Fig. 9. Phase-space Trajectory After Emergency Control - Case 2.

loading decreases, the voltage angle x_2 increases. The system ultimately reaches a long-term equilibrium, as indicated in the figure.

Nevertheless, this is an unstable equilibrium in which oscillations still exist (recall that Case 2 is supposed to fix only the first of the two mentioned issues). The existence of oscillations at the long-term equilibrium is difficult to see in Fig. 9 due to the scaling of the figure. A better way to see that oscillations still exist is presented in Fig. 10. This is the limit cycle on the PLL phase plane at the long-term equilibrium. In this case, a one-second trajectory on the phase plane is plotted, clearly showing the existence of a limit cycle. The oscillatory behavior is clearly visible on the IBR power output, as shown in Fig. 11.

The following sections explore two ways to mitigate the oscillatory behavior of fast dynamics induced by unstable slow dynamics.

C. Case 3 - GFL (Slow PLL) With Voltage Emergency Control

The first method is to reduce the bandwidth of the PLL from 8 Hz to 4 Hz. This is a well-known strategy to reduce

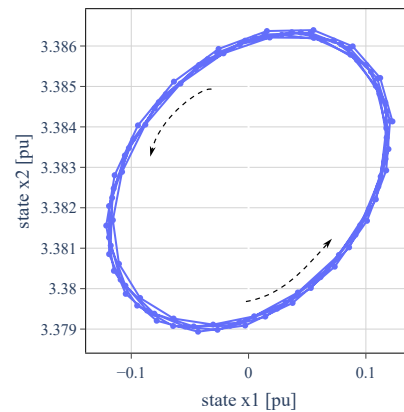


Fig. 10. Limit Cycle After Emergency Control $t = [599, 600]$ - Case 2.

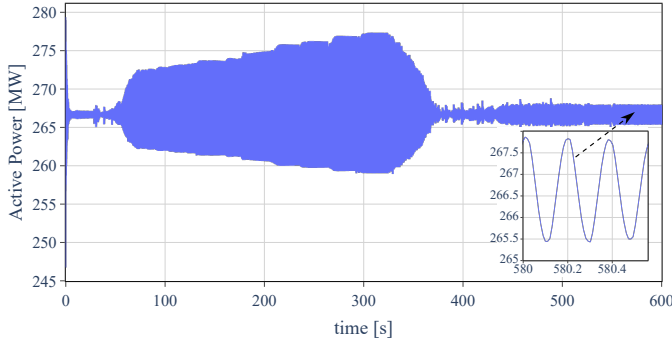


Fig. 11. IBG_6 Active Power - Case 2.

the risk of forced oscillations, although it has its limitations. The evolution of transmission voltages is presented in Fig. 12, in which the oscillatory behavior is no longer perceptible.

To corroborate the non-existence of oscillations, the same trajectory on the phase plane that was presented in Fig. 10 is now superimposed with the results of the case with the 4 Hz-bandwidth PLL (marked as “Slow PLL”). This confirms that the limit cycle disappears and the system reaches a stable long-term equilibrium.

Note that although decreasing the PLL bandwidth improves the dynamic performance in this case, it will slow down the overall control response of the IBR. This requires a compromise between avoiding oscillatory behavior and controller response time so that it meets interconnection requirements, such as rise times. An alternative, more costly, solution is presented in the following section.

D. Case 4 - GFL (Fast PLL) Plus GFM Battery

The IBR_6 represents a photovoltaic generator. While it is tempting to replace its control architecture with GFM control, this may not be a realistic assumption. Most state-of-the-art commercial GFM inverters need some form of energy storage, such as a battery or an HVDC link. Therefore, instead of replacing the existing PV GFL IBR_6, this section considers a 100 MVA GFM battery connected to bus 1042, the same location where the substation transformer of IBG_6 is connected. This section is not a direct comparison between GFL and GFM but intends to provide insights into how GFM technology can

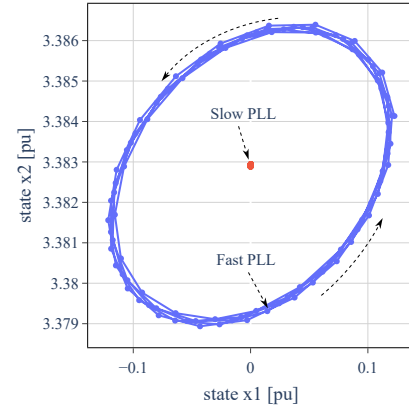


Fig. 13. Limit Cycles $t = [599, 600]$ - Slow PLL (Case 3) and Fast PLL (Case 2).

enhance dynamic performance while still allowing GFL IBRs to operate stably even with a relatively high PLL bandwidth.

The voltage evolution is presented in Fig. 14. By monitoring only transmission voltages, the dynamic performance is very similar to that in Case 3, which simply considered a lower bandwidth PLL without the need for a new GFM battery (a comparison between Figs. 12 and 14 confirms this point). Nevertheless, the solution proposed in Case 3 is known to have limitations in extreme cases of low Short Circuit Ratio (SCR), e.g., $SCR < 1.2$. Case 4 has higher resilience since it considers a new asset that makes it possible to supply 100 MW locally without the need for power transfer through long distances in an N-1 system.

The reactive power of the GFM battery and GFL PV are shown in Fig. 15. It shows that the GFM control overtakes the voltage regulation, with the battery quickly supplying the necessary reactive power support while the GFL IBR keeps its reactive power infeed constant. Once the CVR scheme is activated, the load consumption in the affected area decreases and the GFM battery can reduce its reactive power. In fact, at the end of the emergency control, the battery consumes reactive power to avoid overvoltages, which could be a potential issue with aggressive CVR.

The phase plane trajectory with and without a GFM battery is shown in Fig. 16. For legibility reasons, the trajectory is

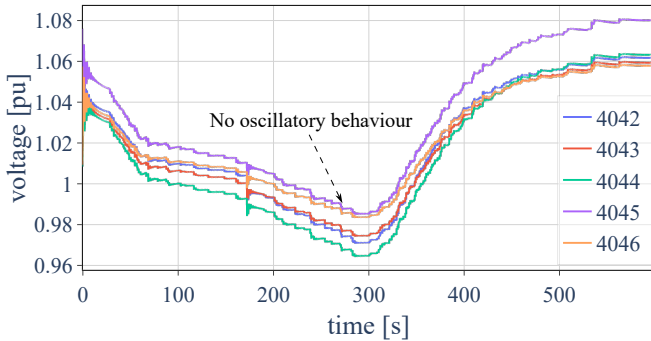


Fig. 12. Evolution of Transmission Voltages - Case 3.

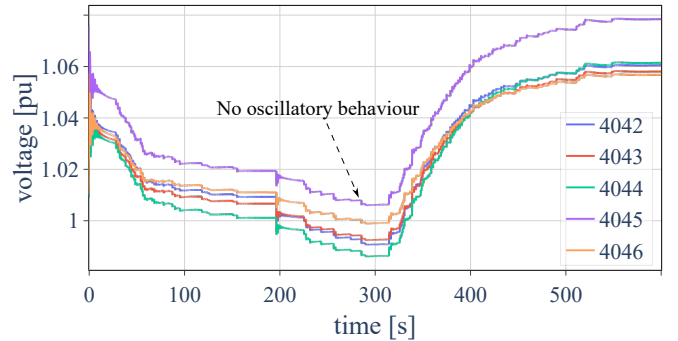


Fig. 14. Evolution of Transmission Voltages - Case 4.

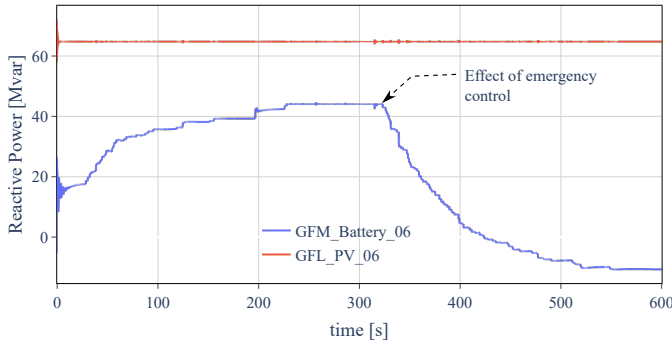


Fig. 15. Reactive Power of GFL and GFM - Case 4.

shown only until the critical point shortly before the OEL of g14 acts. After this point, the CVR will have an effect similar to the one in Fig. 9. The main goal of Fig. 16 is to confirm that both approaches in Cases 3 and 4 avoid the appearance of limit cycles as the long-term dynamics evolve. Case 1 is also shown as a reference.

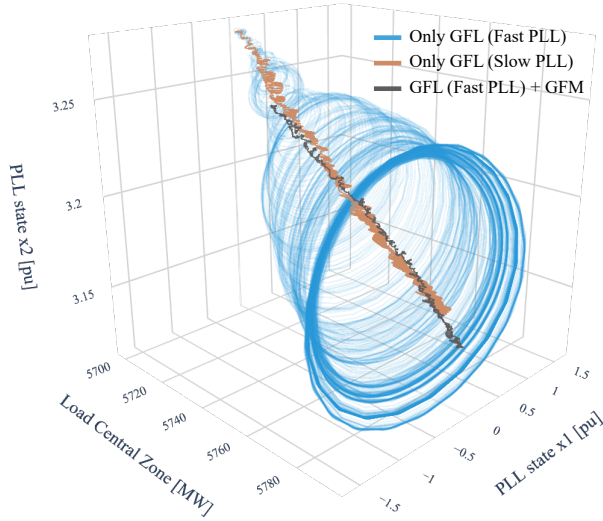


Fig. 16. Phase-space Trajectory With and Without GFM Battery

V. CONCLUSIONS AND FUTURE WORK

Real networks have dynamics that evolve at different time scales and have intrinsic interactions. The dynamics of one time scale can induce instabilities in those of a different time scale. This work highlights the importance of multi-time-scale simulation and exemplifies a case of S-LT3 instability. It shows that the oscillatory behavior of fast IBR dynamics is induced by slower dynamics such as LTCs and OELs. The paper demonstrates that if multi-time-scale simulation is not considered, this instability would be overlooked, and the system could be incorrectly deemed stable. This work also exemplifies how GFM technology can complement GFL controls by enabling stable operation of GFL IBRs without the need to slow down their control response.

This work exclusively used positive-sequence time-domain simulation to confirm that the interaction between slow and fast dynamics is significant even within the time scales that can be captured by this simulation method. While a wider range of dynamics can be captured by EMT simulations, ongoing work by the author utilizes RMS-EMT co-simulation to further investigate crucial interdependencies between dynamics of different time scales.

REFERENCES

- [1] T. Van Cutsem and C. Vournas, *Voltage Stability of Electric Power Systems*, New York, NY, USA: Springer, 1998.
- [2] L. D. Pabon Ospina, "Voltage Stability Assessment and the Need for Multi-Time Scale Dynamic Simulation," in *2025 IEEE PowerTech Conference*, Kiel, Germany, July 2025.
- [3] CIGRE Task Force 38-02-08, *Long term dynamics - phase ii: final report*, CIGRE Publication, 1995.
- [4] IEEE PSDP, "PES-TR9 - Voltage Stability Assessment: Concepts, Practices and Tools," Aug. 2002.
- [5] S. H. Strogatz, *Nonlinear Dynamics and Chaos: With Applications to Physics, Biology, Chemistry, and Engineering*, 2nd ed., CRC Press, 2015.
- [6] S. Chatterjee and S. Geng, "Effects of Line Dynamics on Stability Margin to Hopf Bifurcation in Grid-Forming Inverters," *arXiv preprint arXiv:2412.15449*, 2024.
- [7] IEEE PSDP, "PES-TR19- Test Systems for Voltage Stability Analysis and Security Assessment," *PES-TR19*, 2015.
- [8] L. D. P. Ospina, A. F. Correa, and G. Lammert, "Implementation and validation of the Nordic test system in DiGSILENT PowerFactory," in *2017 IEEE Manchester PowerTech*, June 2017, pp. 1-6.
- [9] IEEE Power & Energy Society, "Power System Dynamic Performance Committee," 2025. [Online]. Available: <https://cmte.ieee.org/pes-psdp/48-9-2/>. [Accessed: Aug. 14, 2025].
- [10] D. Ramasubramanian et al., "Converter Model for Representing Converter Interfaced Generation in Large Scale Grid Simulations," *IEEE Transactions on Power Systems*, vol. 32, no. 1, pp. 765-773, 2017.
- [11] D. Ramasubramanian et al., "Positive sequence voltage source converter mathematical model for use in low short circuit systems," *IET Generation, Transmission & Distribution*, vol. 14, no. 1, pp. 87-97, 2020.
- [12] L. D. Pabón Ospina, D. Pabón Ospina, and V. Usuga Salazar, "Plausibility and Implications of Converter-Driven Oscillations Induced by Unstable Long-Term Dynamics," *IEEE Transactions on Power Systems*, vol. 38, no. 6, pp. 5143-5155, 2023.
- [13] L. D. Pabón Ospina and D. Ramasubramanian, "Grid-Forming and Grid-Following Inverters: A Dynamic Performance Evaluation Using RMS, EMT and Small-Signal Analysis," *CSE (CIGRE Science and Engineering)*, June 2025. [Online]. Available: <https://cse.cigre.org/cs-e-n037/grid-forming-and-grid-following-inverters-a-dynamic-performance-evaluation-using-rms-emt-and-small-signal-analysis.html>.
- [14] Energy Systems Integration Group (ESIG), "GFM Landscape - Modeling and Model Verification Efforts," 2024. [Online]. Available: <https://www.esig.energy/working-users-groups/reliability/grid-forming/gfm-landscape/modeling/>. [Accessed: Aug. 15, 2025].
- [15] Pacific Northwest National Laboratory, "Model Specification of Droop-Controlled, Grid-Forming Inverters (REGFM_A1)," Sept. 2023. [Online]. Available: <https://www.osti.gov/servlets/purl/2229442>.
- [16] L. D. Pabón Ospina and T. Van Cutsem, "Emergency Support of Transmission Voltages by Active Distribution Networks: A Non-Intrusive Scheme," *IEEE Transactions on Power Systems*, vol. 36, no. 5, pp. 3887-3896, 2021.
- [17] L. D. Pabón Ospina and T. Van Cutsem, "Electrical Power System," U.S. Patent 20230231383A1, July 20, 2023. [Online]. Available: <https://patents.google.com/patent/US20230231383A1/en>.
- [18] C. D. Vournas, C. Lambrou, and P. Mandoulidis, "Voltage Stability Monitoring From a Transmission Bus PMU," *IEEE Transactions on Power Systems*, vol. 32, no. 4, pp. 3266-3274, 2017.